materials proceedings

Proceeding Paper

Preparation and Characterization of $NaYF_4$-Based Up-Conversion Nanoparticles for Solar Energy Storage Systems

José Joaquín Manjarrez-Arellano, Miguel A. Hernandez-Martinez, Rubén Caro-Briones, Gabriela Martínez-Mejía, Lazaro Ruiz-Virgen, José Manuel del Río, Miriam Sánchez-Pozos and Mónica Corea

MDPI

https://doi.org/10.3390/materproc2025025016

materials proceedings

MDPI

Proceeding Paper

Preparation and Characterization of $NaYF_4$-Based Up-Conversion Nanoparticles for Solar Energy Storage Systems †

José Joaquín Manjarrez-Arellano [1], Miguel A. Hernandez-Martinez [1], Rubén Caro-Briones [1,2], Gabriela Martínez-Mejía [1], Lazaro Ruiz-Virgen [1], José Manuel del Río [3,4], Miriam Sánchez-Pozos [5] and Mónica Corea [1,*]

[1] Laboratorio de Investigación en Polímeros y Nanomateriales, ESIQIE, Instituto Politécnico Nacional, Av. Luis Enrique Erro S/N, Unidad Profesional Adolfo López Mateos, Zacatenco, Alcaldía Gustavo A. Madero, Ciudad de México 07738, Mexico; jmanjarreza1100@alumno.ipn.mx (J.J.M.-A.); mamtz6046@gmail.com (M.A.H.-M.); rcaro@ipn.mx (R.C.-B.); gamartinezm@ipn.mx (G.M.-M.); lazaro1990@hotmail.com (L.R.-V.)

[2] Escuela Superior de Ingeniería Mecánica y Eléctrica, ESIME, Instituto Politécnico Nacional, Av. Luis Enrique Erro S/N, Unidad Profesional Adolfo López Mateos, Zacatenco, Alcaldía Gustavo A. Madero, Ciudad de México 07738, Mexico

[3] Escuela Superior de Física y Matemáticas, ESFM, Instituto Politécnico Nacional, Av. Luis Enrique Erro S/N, Unidad Profesional Adolfo López Mateos, Zacatenco, Alcaldía Gustavo A. Madero, Ciudad de México 07738, Mexico; jdelriog@ipn.mx

[4] Posgrado en Ciencias en Ingeniería en Metalurgia y Materiales, ESIQIE, Instituto Politécnico Nacional, Av. Luis Enrique Erro S/N, Unidad Profesional Adolfo López Mateos, Zacatenco, Alcaldía Gustavo A. Madero, Ciudad de México 07738, Mexico

[5] Facultad de Ingeniería, Cerro de Coatepec S/N, Universidad Autónoma del Estado de México, Ciudad Universitaria, Toluca de Lerdo 50110, Mexico; msanchezpo@uaemex.mx

* Correspondence: mcoreat@yahoo.com.mx or mcorea@ipn.mx; Tel.: +52-55-57296000 (ext. 55130 or 54239)

† Presented at the 5th International Online Conference on Nanomaterials, 22–24 September 2025; Available online: https://sciforum.net/event/IOCN2025.

Abstract

Up-conversion nanoparticles (UCNPs) are materials that convert near-infrared (NIR) photons into ultraviolet (UV) or visible emissions. To enhance their optical properties, UCNPs are often synthesized with oxide (Y_2O_3) or fluoride ($NaYF_4$) support matrices, useful for energy storage applications. In this study, $NaYF_4$-UCNPs were synthesized via coprecipitation and heat-treated at 400 °C. Then, a tetraethyl orthosilicate (TEOS) film was synthesized by the sol–gel technique at varying pH and temperatures from 25 °C to 80 °C. Characterization using scanning electron microscopy (SEM), X-ray diffraction (XRD), and confocal microscopy (CM) confirmed the up-conversion properties. These materials show promise for enhancing solar radiation density in polymer degradation.

Keywords: nanoparticles; up-conversion properties; solar concentration; polymers; degradation process

Academic Editor: Jose L. Arias Mediano

Published: 18 December 2025

Citation: Manjarrez-Arellano, J.J.; Hernandez-Martinez, M.A.; Caro-Briones, R.; Martínez-Mejía, G.; Ruiz-Virgen, L.; del Río, J.M.; Sánchez-Pozos, M.; Corea, M. Preparation and Characterization of $NaYF_4$-Based Up-Conversion Nanoparticles for Solar Energy Storage Systems. *Mater. Proc.* **2025**, *25*, 16. https://doi.org/10.3390/materproc2025025016

1. Introduction

Nanoparticles (NPs) exhibit unique physicochemical properties, including tunable surface chemistry, nanoscale size (1–1000 nm), controlled morphology, and shape-dependent optical and electronic behaviors in which quantum phenomena such as confinement effects are involved and play a significant role [1–5]. These characteristics make NPs essential in a wide range of fields, including catalysis, sensing, biomedicine, environmental applications, construction, and energy conversion [1–6].

Generally, nanoparticle synthesis methods are classified into three main approaches [7–9]. The physical approach, known as the top-down method, involves breaking down bulk materials into smaller particles. In contrast, the chemical and biological approaches—collectively referred to as bottom-up methods—assemble nanoparticles from atomic or molecular precursors [7–9]. Bottom-up strategies include the coprecipitation method, sol–gel processes, green synthesis, electrospinning, and biochemical routes [7–9].

Specifically, the coprecipitation method is a synthesis process in which two or more compounds (precursors) are precipitated simultaneously in a solvent [8,10,11]. Coprecipitation occurs as a result of supersaturation, during which the nucleation, growth, and agglomeration of nanoparticles take place in a specific solution [8,10,11]. The most critical step in coprecipitation is nucleation (particle formation), after which secondary processes such as Ostwald ripening and aggregation occur [8,10,11]. These secondary processes strongly influence the particle size, morphology, and overall properties of the final nanoparticles [8,10,11]. Parameters such as the rate of reactant addition, pH, temperature, and stirring conditions play key roles in determining the particle size distribution, morphology, and structure of nanoparticles [8,10–12]. The sol–gel process involves two main steps: hydrolysis (reaction with water) and condensation (polymerization and linkage of molecules) of precursor compounds to form a solid network [13,14]. This method can be conducted under acidic or basic conditions, which significantly influence the properties of the final materials [13,14]. For sol–gel synthesis, tetraethyl orthosilicate (TEOS) is the silicate precursor most commonly employed, while water and/or ethanol are typically used as solvents [13,14]. The process begins with the formation of a sol, which is a colloidal suspension of solid particles in a liquid. Finally, the sol is transformed into a gel, which is a three-dimensional network [13,14].

In this context, up-conversion nanoparticles (UCNPs) are materials that convert low-energy infrared photons into higher-energy visible or ultraviolet emissions [15,16]. This process occurs via sequential absorption and energy transfer between doped lanthanide ions (Eu, Tb, Tm) in a host lattice [15,16]. However, to optimize the performance of UCNPs, they are often supported or coated with silica matrices derived from TEOS through sol–gel process emissions (Figure 1) [15,16]. The combination of the optical advantages of UCNPs with the chemical stability of silica not only enhances energy conversion efficiency but also ensures the durability and stability of the UCNPs under operational conditions in solar applications [15,16].

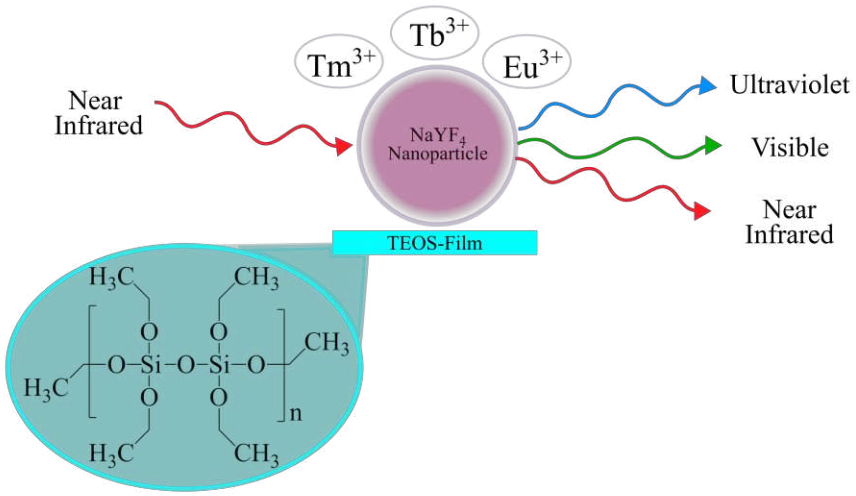

Figure 1. Schematic representation of $NaYF_4$ up-conversion nanoparticles embedded in a TEOS film. The red arrow indicates infrared radiation, the blue arrow indicates ultraviolet radiation, and the green arrow indicates visible radiation.

In this study, up-conversion nanoparticles (UCNPs) were synthesized via coprecipitation and heat-treated at 400 °C for 15 h and 17 h, respectively. Additionally, TEOS-based sol–gel solutions were prepared at different pH values and deposited onto glass substrates using the dip-coating technique, followed by thermal treatment at 450 °C. The results reveal that UCNPs treated for 15 h exhibit more defined morphological features and stronger emission peaks than those treated for 17 h. Moreover, TEOS films prepared at pH = 3 display a porous structure, while films at pH = 5 show an irregular, granular surface. These findings emphasize the significance of optimizing treatment time and pH of medium for controlling material properties and enhancing up-conversion luminescence. Finally, the materials demonstrated high potential for use in solar concentration systems, offering a promising approach for enhancing energy conversion efficiency.

2. Materials and Methods

Two sets of up-conversion nanoparticles (UCNPs) heat-treated for 15 and 17 h, respectively, were synthesized via coprecipitation. In addition, TEOS films were prepared at different pH values using the sol–gel method, as described below. The chemicals used in this research are summarized in Table 1. All reagents were used as received without further purification. Distilled water was deionized using a Barnstead Micropure water purification system (Thermo Fisher Scientific Inc., Niederelbert, Germany).

Table 1. Chemical specifications.

Chemicals	Source and Country	Molecular Weight (Mw) and Mass Fraction Purity	CAS No
Sodium fluoride (NaF)	Sigma-Aldrich; Bangalore; India.	Mw ~ 41.99 g mol^{-1}; ≥ 99.0%	7681-494
Ethylenediaminetetraacetic acid (EDTA)	J.T. Baker; Mexico City; Mexico.	Mw ~ 372.24 g mol^{-1}; ≥ 99.99%	6381-92-6
Tetraethyl orthosilicate (TEOS)	Sigma-Aldrich; Wuxi City; China.	Mw ~ 208.33 g mol^{-1}; ≥ 98.0%	78-10-14
Yttrium oxide (Y_2O_3)	Sigma-Aldrich; Wuxi; China.	Mw ~ 225.81 g mol^{-1}; ≥ 99.99%	1314-36-9
Thulium oxide (Tm_2O_3)	Sigma-Aldrich; Urbana; USA.	Mw ~ 385.87 g mol^{-1}; ≥ 99.99%	12036-44-1
Ytterbium oxide (Yb_2O_3)	Sigma-Aldrich; Wuxi; China.	Mw ~ 394.08 g mol^{-1}; ≥ 99.99%	1314-37-0
Hydrochloric acid (HCl)	Herschi Trading; Mexico City; Mexico.	Mw ~ 36.46 g mol^{-1}; ≥ 36.50% [a]	7647-01-0
Distilled water (H_2O)	Isse Labs. S.A. de C.V.; López Mateos City; Mexico.	Mw ~ 18.02 g mol^{-1}; [a]	7732-18-5
Ethanol (C_2H_5OH)	D'Mik; Los Reyes Acaquilpan; Mexico.	Mw ~ 46.07 g mol^{-1}; ≥ 96.0%	64-17-5

[a] Industrial grade.

2.1. Synthesis of Sodium Yttrium Fluoride ($NaYF_4$) Nanoparticles and TEOS Films

2.1.1. Synthesis of $NaYF_4$ Up-Conversion Nanoparticles

The formulation of $NaYF_4$ up-conversion nanoparticles is shown in Table 2. The synthesis was carried out in four steps as shown in Figure 2: (1) Yttrium oxide (Y_2O_3), thulium oxide (Tm_2O_3), and ytterbium oxide (Yb_2O_3) were each dissolved separately in concentrated hydrochloric acid (HCl). (2) The rare-earth chloride solutions were then added dropwise to an aqueous solution of sodium fluoride (NaF) under continuous stirring. Subsequently, ethylenediaminetetraacetic acid (EDTA) dissolved in HCl was introduced as a surfactant, and the mixture was maintained under constant stirring for 1 h at 25 °C. (3) After the reaction, the obtained solutions were washed in an Eppendorf Centrifuge 800D (Shanghai, China) for 10 min at 4000 RPM using deionized water and ethanol in triplicate, and the supernatant was decanted. (4) Finally, two sets of up-conversion nanoparticles

(UCNPs) were heat-treated in a Nabertherm Muffle Furnace (Lilienthal, Germany) at 400 °C for 15 h and 17 h under a nitrogen atmosphere.

Table 2. Formulation of $NaYF_4$ up-conversion nanoparticles.

Compounds	Mass (g)				
Yttrium oxide (Y_2O_3)	0.3				
Thulium oxide (Tm_2O_3)		0.015			
Ytterbium oxide (Yb_2O_3)			0.1		
Ethylenediaminetetraacetic acid (EDTA)				1.1	
Hydrochloric acid (HCl)	8.0	0.3	3.4	10	
Sodium fluoride (NaF)					1
Distilled water (H_2O)					30

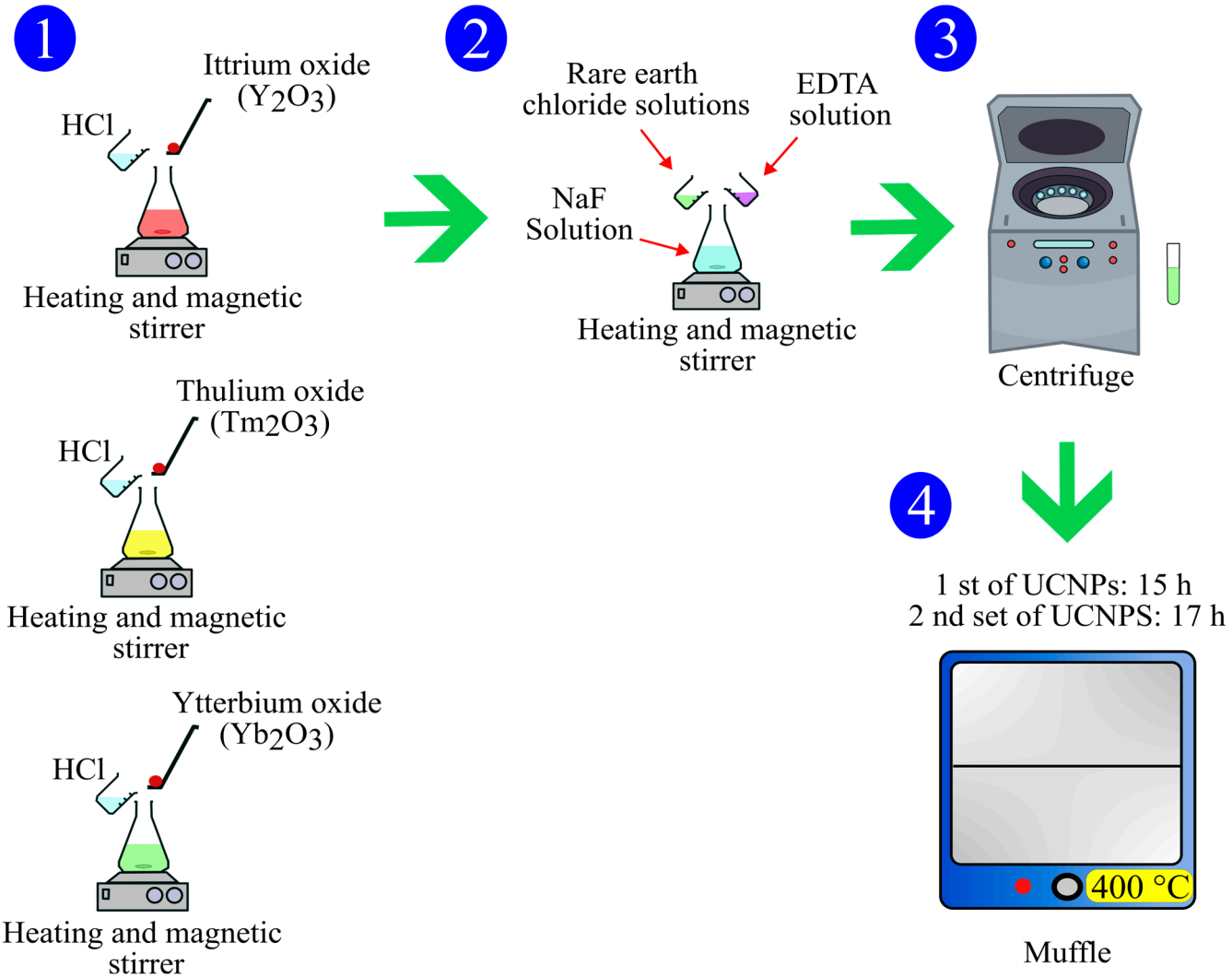

Figure 2. Synthesis route of $NaYF_4$ up-conversion nanoparticles.

2.1.2. Synthesis of Tetraethyl Orthosilicate (TEOS) Films

The synthesis was carried out in three steps as shown in Figure 3. For step 1, three different solutions containing tetraethyl orthosilicate (TEOS), deionized water (H_2O), and ethanol (C_2H_5OH) in a molar ratio of 1:4:15 were prepared and placed in round-bottom flasks. The pH values of solutions were adjusted to 5 and 3 by adding concentrated hydrochloric acid (HCl), and measured using a Conductronic PC45 pH meter (Puebla, Mexico). The mixtures ($TEOS/H_2O/C_2H_5OH$) were stirred using a Thermo Scientific

heating magnetic stirrer (Waltham, MA, United States) at 25, 70, 75, and 80 °C for 1 h. For step 2, film preparation, glass substrates were cleaned and coated using the dip-coating technique. Finally, during the step 3, the obtained films were subjected to thermal treatment in a Nabertherm Muffle Furnace (Lilienthal, Germany) at 450 °C for 1 h.

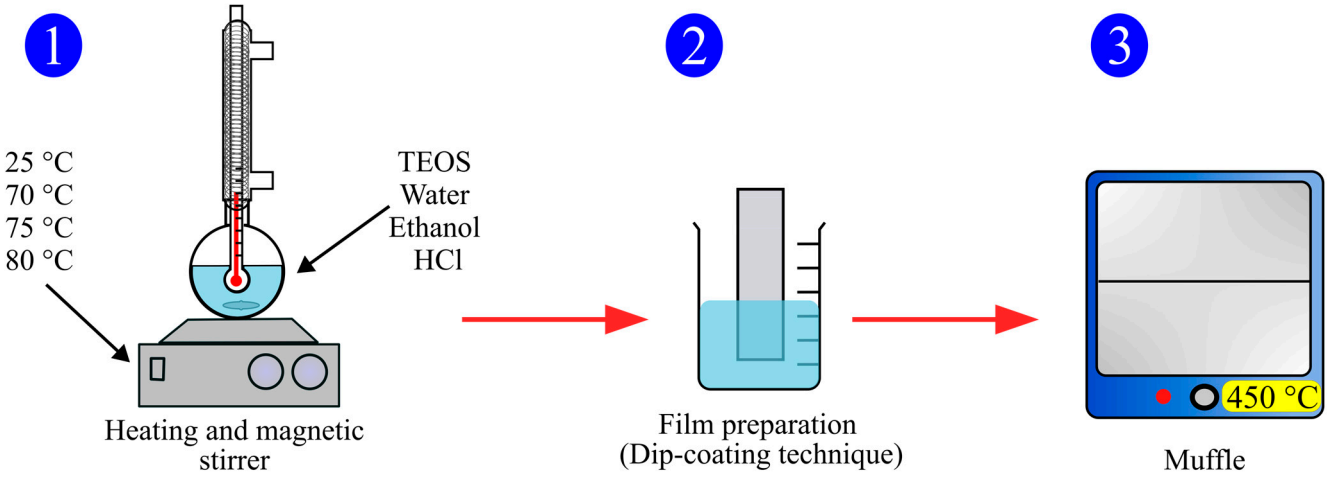

Figure 3. Synthesis route of tetraethyl orthosilicate (TEOS) films.

2.2. Characterization of (Sodium Yttrium Fluoride) $NaYF_4$ Nanoparticles and TEOS Films

2.2.1. Scanning Electron Microscopy (SEM)

The surface morphology and structure of $NaYF_4$ up-conversion nanoparticles and TEOS films were analyzed using a scanning electron microscope JEOL JSM 6400 (Tokyo, Japan). Each sample was deposited on a separate sample holder without prior dilution. $NaYF_4$ nanoparticles and TEOS films were coated with a thin gold layer using an SPI-Module™ Sputter Coater (West Chester, PA, USA) for 2 s. SEM analyses were performed under the following operating conditions: magnifications ranging from 100× to 35,000×, a working distance (WD) of 7–10 mm, and an accelerating voltage of 10 kV.

2.2.2. X-Ray Diffraction (XRD)

The diffractograms of $NaYF_4$ up-conversion nanoparticles were obtained by the X-ray diffractometer from Rigaku model Miniflex 600 (Tokyo, Japan). The diffraction angle 2θ was from 20 to 80°, the X-ray tube was made of Cu, the intensity was 15 mA, and the voltage was 40 kV. The samples were analyzed in powder form at room temperature.

2.2.3. Multiphoton Confocal Microscopy (CM)

Confocal imaging of $NaYF_4$ up-conversion nanoparticles (UCNPs) was performed using a multiphoton confocal microscope LSM 710 NLO (Carl Zeiss, Jena, Germany) equipped with a multiphoton laser operating in the range of 690–1090 nm. Excitation wavelengths of 405, 488, 561, and 633 nm were used to record the up-conversion emission signals. Prior to analysis, the powders were ground in a mortar to ensure homogeneity. Approximately 0.1 g of each sample was placed directly onto a glass slide for measurement without further treatment.

3. Preliminary Results

3.1. Characterization of $NaYF_4$ Up-Conversion Nanoparticles with Different Heat-Treatment Times and TEOS Films Synthesized at Various pH Values and Temperatures

3.1.1. Scanning Electron Microscopy (SEM) of $NaYF_4$ Up-Conversion Nanoparticles

Figure 4 shows the SEM images of two sets of $NaYF_4$ nanoparticles heat-treated for different times: (a) 15 h and (b) 17 h. In Figure 4a, the particles exhibit a partially spherical

morphology, irregular surfaces, and a small size. In contrast, the nanoparticles treated for 17 h presented irregular surfaces and increased agglomeration, as shown in Figure 4b. This behavior is due to Ostwald ripening and phase transformation [8,17]. This process is a common phenomenon in nanocrystal synthesis and depends on several factors such as temperature, reaction time, and initial precursor materials [8,17].

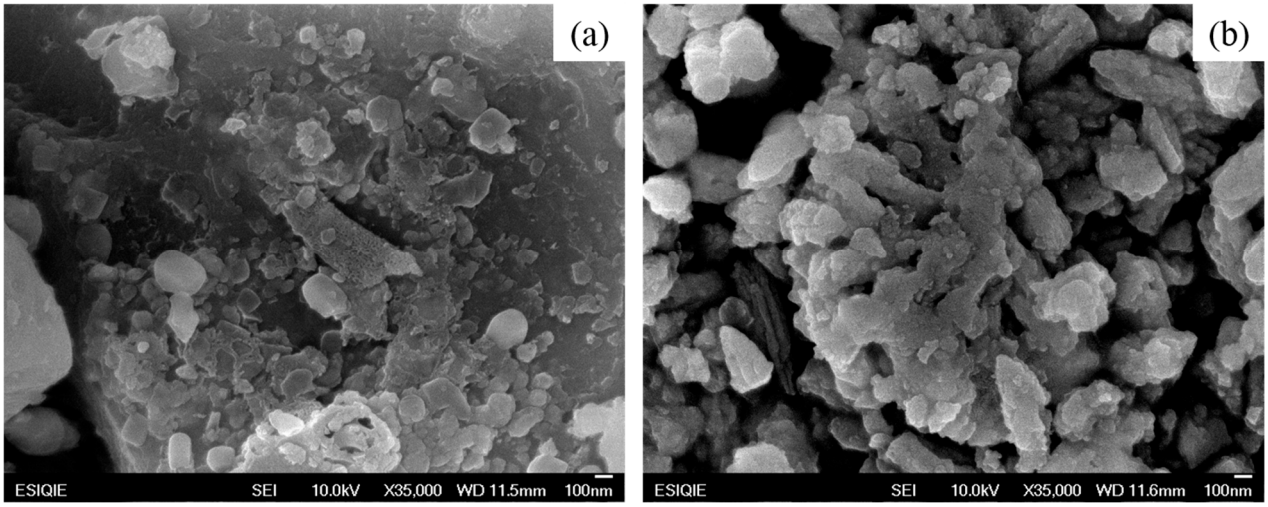

Figure 4. SEM images of $NaYF_4$ up-conversion nanoparticles heat-treated for (**a**) 15 h and (**b**) 17 h.

3.1.2. X-Ray Diffraction (XRD) Spectra of $NaYF_4$ Up-Conversion Nanoparticles

XRD spectra of $NaYF_4$ up-conversion nanoparticles heat-treated for different times ((a) 15 h and (b) 17 h) are shown in Figure 5. The characteristic peaks are observed at 2θ ≈ 27.1°, 29.48°, 35.96°, 39.78°, 44.9°, 48.12°, 51.1°, 55.46°, 56.42°, and 58.30° [18,19]. These peaks correspond to the Miller indices (110), (101), (200), (111), (201), (210), (002), (300), (211), and (102), respectively [18,19]. The presence of these peaks confirms the hexagonal β-phase of $NaYF_4$ UCNPs [18,19], because this phase favors the up-conversion properties.

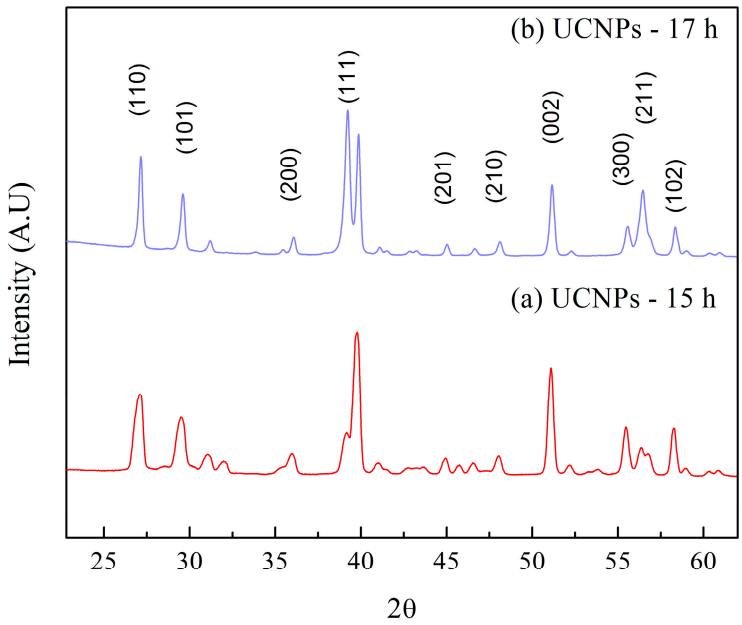

Figure 5. XRD spectra of $NaYF_4$ up-conversion nanoparticles after heat treatment for (**a**) 15 h and (**b**) 17 h.

3.1.3. Multiphoton Confocal Microscopy (CM) of NaYF4 Up-Conversion Nanoparticles

Figure 6a,b shows the emission spectra of $NaYF_4$ up-conversion nanoparticles after heat treatment for (a) 15 h and (b) 17 h, respectively. The $NaYF_4$ UPCNs treated for 15 h exhibit more defined emission peaks compared to those treated for 17 h. This difference can be attributed to the process of up-conversion luminescence, which occurs when $NaYF_4$ nanoparticles doped with specific lanthanide ions absorb multiple low-energy photons (typically in the near-infrared range) and emit a single higher-energy photon in the UV-Vis spectrum [20].

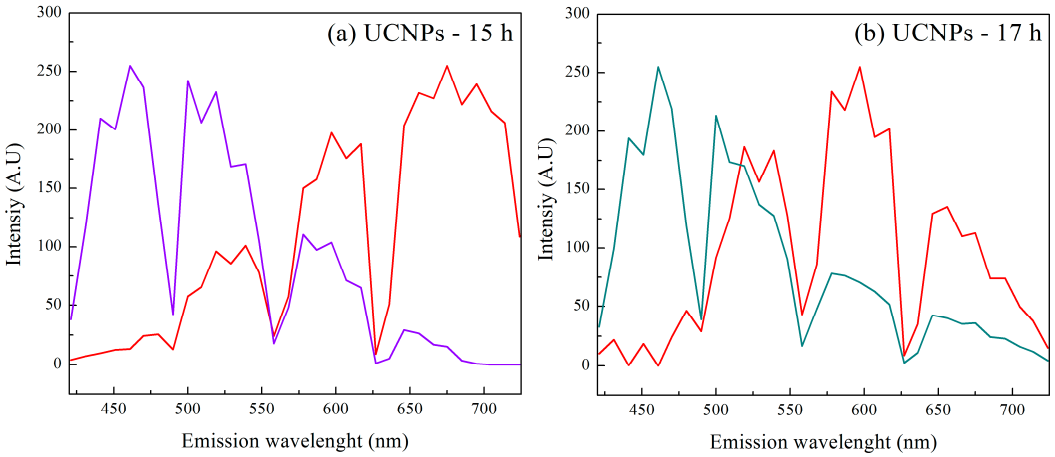

Figure 6. Emission spectra of $NaYF_4$ up-conversion nanoparticles after heat treatment for (**a**) 15 h and (**b**) 17 h. Red lines correspond to absorption peaks, while green and purple lines correspond to emission peaks, respectively.

3.1.4. Scanning Electron Microscopy (SEM) of TEOS Film Synthesized at Different pH and Temperatures

Figure 7 shows the SEM images of TEOS films synthesized at pH values of 3 and 5 at 75 °C and 80 °C, as examples. At a pH of 3, the TEOS films obtained a porous structure. However, at pH = 5, the surface became more irregular and granular, and the porous structure of the film decreased. This behavior can be attributed to the sol–gel process carried out at different pH conditions. This means that, in an acid-catalyzed environment (pH 3), hydrolysis predominates, whereas in an environment with a pH of 5, condensation occurs more efficiently [21,22].

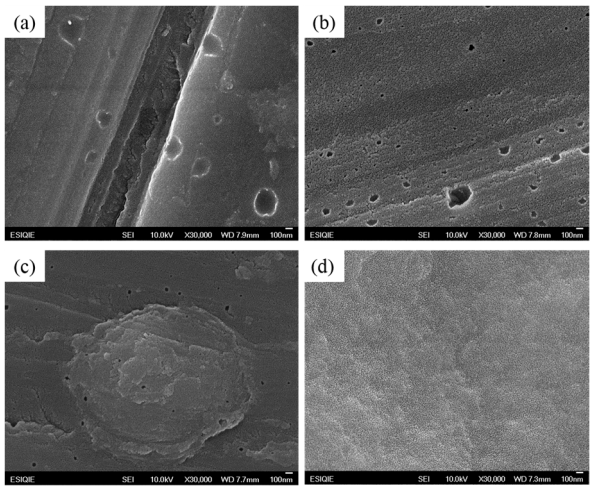

Figure 7. SEM images of TEOS films synthesized at pH values of 3 and 5 at (**a**,**b**) 75 °C and (**c**,**d**) 80 °C, respectively.

4. Conclusions

$NaYF_4$ nanoparticles treated for 15 h show more defined morphologies and stronger emission than those treated for 17 h. TEOS films formed at pH 3 are porous, whereas those at pH 5 exhibit irregular, granular surfaces due to different sol–gel mechanisms. These results confirm the strong effect of treatment time and pH on structural and optical behavior. Overall, the materials present promising potential for use in solar concentration systems and improved energy conversion efficiency.

Author Contributions: Conceptualization, J.J.M.-A., L.R.-V., J.M.d.R., M.S.-P., and M.C.; methodology, J.J.M.-A., L.R.-V., and M.C.; software, J.J.M.-A., M.A.H.-M., and L.R.-V.; validation, J.J.M.-A., M.A.H.-M., G.M.-M., R.C.-B., L.R.-V., J.M.d.R., and M.C.; formal analysis, G.M.-M., R.C.-B., L.R.-V., J.M.d.R., and M.C.; investigation, J.J.M.-A., L.R.-V., and M.C.; resources, J.J.M.-A., L.R.-V., and M.C.; data curation, J.J.M.-A., G.M.-M., R.C.-B., L.R.-V., J.M.d.R., M.S.-P., and M.C.; writing—original, J.J.M.-A., M.A.H.-M., G.M.-M., R.C.-B., L.R.-V., J.M.d.R., M.S.-P., and M.C.; writing—review and editing, L.R.-V., J.M.d.R., M.S.-P., and M.C.; visualization, J.J.M.-A., L.R.-V., J.M.d.R., and M.C.; supervision, G.M.-M., R.C.-B., L.R.-V., J.M.d.R., M.S.-P., and M.C.; project administration, J.M.d.R. and M.C.; funding acquisition, J.M.d.R. and M.C. All authors have read and agreed to the published version of the manuscript.

Funding: This research received no external funding.

Institutional Review Board Statement: Not applicable.

Informed Consent Statement: Not applicable.

Data Availability Statement: The dataset is available from the authors upon request.

Acknowledgments: The authors gratefully acknowledge the support provided by the Instituto Politécnico Nacional (IPN) and Centro de Nanociencias y Micro-Nanotecnologías (IPN-CNMN).

Conflicts of Interest: The authors declare no conflicts of interest.

References

1. Abdolhosseini, M.; Zandsalimi, F.; Moghaddam, F.S.; Tavoosidana, G. A review on colorimetric assays for DNA virus detection. *J. Virol. Methods* **2022**, *301*, 114461. [CrossRef] [PubMed]
2. Ruiz-Virgen, L.; Hernández-Martínez, M.A.; Martínez-Mejía, G.; Caro-Briones, R.; del Río, J.M.; Corea, M. Study of Thermodynamic and Rheological Properties of Sensitive Polymeric Nanoparticles as a Possible Application in the Oil Industry. *J. Solut. Chem.* **2024**, *53*, 5–27. [CrossRef]
3. Ruiz-Virgen, L.; Hernández-Martínez, M.A.; Martínez-Mejía, G.; Caro-Briones, R.; Herbert-Pucheta, E.; el Río, J.M.; Corea, M. Analysis of Structural Changes of pH–Thermo-Responsive Nanoparticles in Polymeric Hydrogels. *Gels* **2024**, *10*, 541. [CrossRef] [PubMed]
4. Arora, N.; Manchanda, H.; Gupta, M. Recent advances in green synthesis, characterization and emerging applications of nanoparticles and derived nanofluids. *Renew. Sustain. Energy Rev.* **2026**, *226*, 116354. [CrossRef]
5. Nadeem, J.; Dirk, L. Nanoparticle classification, physicochemical properties, characterization, and applications: A comprehensive review for biologists. *J. Nanobiotechnol.* **2022**, *20*, 262. [CrossRef]
6. Chen, G.; Qiu, H.; Prasad, P.N.; Chen, X. Upconversion Nanoparticles: Design, Nanochemistry, and Applications in Theranostics. *Chem. Rev.* **2014**, *114*, 5161–5214. [CrossRef] [PubMed]
7. Wu, X.; Chen, G.; Shen, J.; Li, Z.; Zhang, Y.; Han, G. Upconversion Nanoparticles: A Versatile Solution to Multiscale Biological Imaging. *Bioconjugate Chem.* **2015**, *26*, 166–175. [CrossRef] [PubMed]
8. Pineda-Sánchez, R.; Martinez-Calvo, E.A.; Sánchez-Pozos, M.; Corea, M. Review on polymer degradation by selective solar concentration using up-conversion nanoparticles. *J. Polym. Res.* **2023**, *30*, 296. [CrossRef]
9. Vijay, K.; Irfan, A.; Hendrik, C.S.; Rakesh, S. *Upconversion Nanoparticles (UCNPs) for Functional Applications*, 1st ed.; Springer: Singapore, 2023; pp. 1–465.
10. Khalid, H.; Chaudhry, A.A. Basics of Hydroxyapatite Structure, Synthesis, Properties, and Clinical Applications. In *Biomedical Materials: Advances and Applications*, 2nd ed.; Smith, J., Doe, R., Eds.; Springer: Berlin, Germany, 2020; Volume 4, pp. 154–196.

11. Varanda, L.C.; Souza, C.G.S.d.; Perecin, C.J.; Moraes, D.A.d.; Queiróz, D.F.d.; Neves, H.R.; Souza Junior, J.B.; Silva, M.F.d.; Albers, R.F.; Silva, T.L.d. Inorganic and Organic–Inorganic Composite Nanoparticles with Potential Biomedical Applications: Synthesis Challenges for Enhanced Performance. In *Materials for Biomedical Engineering: Bioactive Materials, Properties, and Applications*, 1st ed.; Grumezescu, V., Grumezescu, A.M., Eds.; Elsevier: Amsterdam, The Netherlands, 2019; pp. 47–99.
12. Yang, Z.; Xia, Z. Ceramics Phosphor Powders. In *Advanced Ceramics for Energy Storage, Thermoelectrics and Photonics*; Elsevier Series in Advanced Ceramic Materials; Cao, P., Chen, Z.-g., Xia, Z., Eds.; Elsevier: Amsterdam, The Netherlands, 2023; pp. 395–429.
13. Zheng, K.; Boccaccini, A.R. Sol-gel processing of bioactive glass nanoparticles: A review. *Adv. Colloid Interface Sci.* **2017**, *249*, 363–373. [CrossRef] [PubMed]
14. Larry, L.; HenchJon, K.W. The sol-gel process. *Chem. Rev.* **1990**, *90*, 33–72. [CrossRef]
15. Saheb Naher, H.; Al-Turaihi, B.A.H.; Mohammed, S.H.; Naser, S.M.; Albark, M.A.; Madlool, H.A.; Al-Marzoog, H.A.M.; Jalil, A.T. Upconversion Nanoparticles (UCNPs): Synthesis Methods, Imaging and Cancer Therapy. *J. Drug Deliv. Sci. Technol.* **2023**, *80*, 104175. [CrossRef]
16. Wen, S.; Zhou, J.; Zheng, K. Advances in highly doped upconversion nanoparticles. *Nat. Commun.* **2018**, *9*, 2415. [CrossRef] [PubMed]
17. Beien, Z.; Rui, Q.; Lina, Y.; Yi, G. Real-time atomistic simulation of the Ostwald ripening of TiO_2 supported Au nanoparticles. *Nanoscale* **2020**, *12*, 19142–19148. [CrossRef]
18. Wei, Y.; Lu, F.; Zhang, X.; Chen, D. Synthesis and characterization of efficient near-infrared upconversion Yb and Tm codoped $NaYF_4$ nanocrystal reporter. *Alloys Compd.* **2007**, *427*, 333–340. [CrossRef]
19. Li, H.; Shi, X.; Li, X.; Zong, L. Size-tunable β-$NaYF_4$:Yb/Er up-converting nanoparticles with a strong green emission synthesized by thermal decomposition. *Opt. Mater.* **2020**, *108*, 110144. [CrossRef]
20. Chen, C.; Wang, F.; Wen, S.; Su, Q.P.; Wu, M.C.; Liu, Y.; Wang, B.; Li, D.; Shan, X.; Kianinia, M.; et al. Multi-photon near-infrared emission saturation nanoscopy using upconversion nanoparticles. *Nat. Commun.* **2018**, *9*, 3290. [CrossRef] [PubMed]
21. Darmawan, A.; Munzakka, L.; Karlina, L.; Saputra, R.E.; Sriatun, S.; Astuti, Y.; Wahyuni, A.S. Pervaporation membrane for desalination derived from tetraethylorthosilicate-methyltriethoxysilane. *J. Sol-Gel Sci. Technol.* **2022**, *101*, 505–518. [CrossRef]
22. Chang, K.-C.; Chen, Y.-K.; Chen, H. Fabrication of highly transparent and superhydrophobic silica-based surface by TEOS/PPG hybrid with adjustment of the pH value. *Surf. Coat. Tech.* **2008**, *202*, 3822–3831. [CrossRef]